Theoretical and Experimental Study of Photonic Crystal Based Structures for Optical Communication Applications

Wei Jiang[*a,b], Jizuo Zou[a], Linghui Wu[b], Yihong Chen[b], Chuhua Tian[a], Brie Howley[a], Xuejun Lu[c], and Ray T. Chen[a,b]

[a]Microelectronics Research Center and Department of Electrical and Computer Engineering, University of Texas, Austin, Texas 78758
[b]Omega Optics, 10435 Burnet Road, Suite 108, Austin, Texas 78758
[c]Department of Electrical and Computer Engineering, University of Massachusetts, Lowell, MA 01854

ABSTRACT

Photonic crystal based structures have been considered for optical communication applications. A class of novel symmetric structures consisting of cavities and waveguides have been proposed to serve as optical add-drop multiplexers. Light transfer processes in these structures are analyzed briefly. The problem of deviating from the perfect accidental degeneracy is addressed for practical designs, and the backscattering intensities are shown low for the slight deviations. Anomalous light refraction at a surface of a photonic crystal has also been studied. The limitations of prior theoretical methods for the transmission problem are discussed. An outline of a new analytic theory that overcomes these limitations is presented. Photonic crystals are fabricated on polymer multi-layer films and integrated with conventional channel waveguides.

Keywords: photonic crystal, optical add-drop multiplexer, wavelength-division-multiplexing, backscattering, superprism effect, polymer waveguide

1. INTRODUCTION

Photonics research has prospered in the last decade, owing to the rise of wavelength-division-multiplexing(WDM) technology in fiber-optic communications. In recent years, more and more photonics research has shifted toward the direction of nano-structure design and fabrication, with photonic crystals[1,2] regarded as one of the promising approaches in a broad range of applications. Photonic crystals are a new class of artificial optical materials with periodic dielectric structures, which result in unusual optical properties[3-5] that can provide a revolutionary solution for many problems.

This paper covers a range of photonic crystal research activities in the Optical Interconnect group at the University of Texas at Austin. In addition, this paper will explore or explain, in certain detail, some important issues in a number of topics of photonic crystal study. These issues are left out in the literature, yet the complete understanding of these issues, as we shall see, is necessary for furthering the research in these topics.

2. OPTICAL ADD-DROP MULTIPLEXERS BASED ON PHOTONIC CRYSTAL WAVEGUIDES AND CAVITIES

2.1 Photonic crystal based cavities and waveguides

Photonic crystals are a class of novel materials that offer new opportunities for the control and manipulation of light. These materials are composed of a periodic array of microscopic low-dielectric-constant scatterers in a homogeneous high-dielectric-constant background, or high-dielectric-constant

---

[*] jiang@ece.utexas.edu; phone 1-512-471-2003; fax 1-512-471-8575.

scatterers in a homogeneous low-dielectric-constant background. For example, a single slab of semiconductor (high dielectric constant) that hosts a periodic array of air-holes (low dielectric constant). The underlying concept of photonic crystals originates from two seminal papers by Yablonovitch[1] and John[2], respectively. The basic idea is to engineer a structure so that it manipulates the properties of photons in essentially same way that regular crystals affect the properties of electrons. Electrons in a regular crystal see a periodic array of atoms, the coherent scattering felt by the electrons of this array will prevent an electron from traveling in the solid if the energy of the electron unfortunately falls into certain ranges. Each separate energy range of such property is called an energy gap. By the same token, a photonic band gap exists for photons in a photonic crystal in a range of frequencies where light is forbidden to travel within the photonic crystal regardless of its direction of propagation. Such a bandgap renders a photonic crystal an omni-directional mirror that reflects incident light in any direction.

If a point defect is nevertheless formed in a photonic crystal, the omni-directional mirroring effect will confine light around the defect to a small volume that is comparable to wavelength[2], resulting in an optical cavity of high optical energy density and high quality factor. Employing such novel photonic crystal cavities, significant advances have been achieved in semiconductor quantum-well lasers[3] and quantum-dot lasers[4]. Meanwhile, photonic crystal waveguides have been extensively studied recently. Photonic crystal waveguides are essentially one-dimensional defects created inside a photonic crystal by removing a row of "atoms." Photonic crystal waveguides first aroused a significant interest of research community after the theoretical[5] and experimental[6] demonstration of a sharp 90° waveguide bend with almost zero bending loss. However, recent progress of photonic crystal waveguides more and more focuses on the extremely high dispersion capability of photonic crystal waveguides, which has a wider range of applications in light amplification, wavelength conversion,[7] and dispersion compensation.[8] By certain special design of photonic crystal waveguides, the dispersion D(delay difference of optical pulses per unit wavelength deviation per propagation distance) can reach up to 10^5 times larger than the value of regular dispersion compensation fibers.[7] The high dispersion of the photonic crystal waveguides have been carefully demonstrated and characterized experimentally. Excellent agreement between theoretical prediction and experiment dispersion curve has been confirmed and made-to-order dispersion are shown achievable with careful design and fabrication.[7]

2.2 Optical Add drop multiplexers

Using photonic crystal based cavities and waveguides as building blocks, infinite opportunities in novel device configurations have emerged. One of such devices is a channel drop filter that selectively drop one specific wavelength from a broadband incoming light in a waveguide. [9-10] Such devices are usually called Optical Add-Drop Multiplexers(OADM) in WDM optical communications. The originally proposed structures have one or two pairs of cavities symmetrically placed between two parallel waveguides. The working principle is that when the frequency of the light is close to the resonant frequencies of the cavities, light in one of the waveguides will be coupled to the cavity modes through evanescent tails in the waveguide cladding, and be further coupled into the other waveguide. By careful design, 100% light transfer to the other waveguide is shown possible.

In a recent letter, we have discussed the light drop processes in a more general situation, where n waveguides and n pairs of cavities are arranged in an n-fold symmetric structure.[11] Such a structure is characterized by a group C_{nv}. A structure for $n=3$ is shown in Fig. 1. The analysis of these structure is considerably more difficult than that of the original structures, which correspond to a case of $n=2$. Group theory indicates that for $n>2$, the group C_{nv} is generally not an abelian group.[12,13] This means that the symmetry operations of the group C_{nv} do not commute with each other; therefore, irreducible representations of dimensions higher than unity appear. As a consequence, a fundamental difficulty in analysis arises in that there is not a set of basis functions that are eigenfunctions of all symmetry operations. Consider the Hamiltonian of such a system

$$H = H_0 + V,$$

$$H_0 = \sum_{m=0}^{n-1}\sum_{k}\omega_k |mk\rangle\langle mk| + \sum_{m=0}^{n-1}\sum_{k}\omega_{mc}|mc\rangle\langle mc|, \tag{1}$$

$$V = \sum_{m,m'c,c'}(1-\delta_{mm'}\delta_{cc'})|mc\rangle\langle m'c'| + \sum_{m,m'k,c}\left[V_{mc,m'k}|mc\rangle\langle m'k| + V_{m'k,mc}|m'k\rangle\langle mc|\right],$$

where $|mk\rangle$ is a propagating mode with wavevector k and frequency ω_k in waveguide m, The mode $|mc\rangle$ is a localized mode of the resonator pair next of waveguide mode m, $c=e,\ o$ for the even and odd modes, respectively; ω_k is its frequency. The coefficients $V_{mc,m'c'}$ and $V_{mc,m'k}$ represent the coupling between the corresponding modes. We have neglected the coupling between the propagating modes of different waveguides as discussed by Xu et. al.[14]
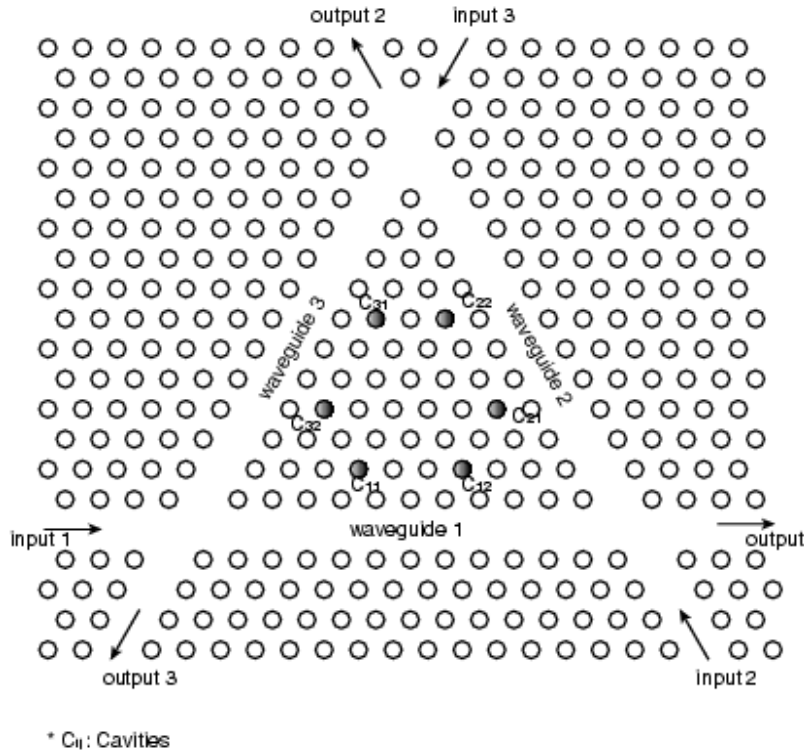

Fig. 1 Schematic drawing of an $n=3$ symmetric OADM that consists of cavities and waveguides.

If we follow the standard group theoretical approach and choose a basis function according irreducible representations, the problem becomes extremely difficult to analyze. The hardest part lies in constructing a mode that has zero backscattering amplitude, which is required for an ideal OADM. Our experiences with a number of basis functions have shown that the following choice offers the most convenience in the study

$$|\alpha k\rangle = \frac{1}{\sqrt{n}}\sum_{m=0}^{n-1}e^{i\frac{2\pi}{n}\alpha m}|mk\rangle, \quad \alpha = 0,1,...,n-1. \tag{2}$$

One easily sees this is an eigenfunction of the rotation operator C_n, although when the mirror operator applies to it, the resultant state will be indexed by $\bar{\alpha}$ rather than by α. We can easily show that the Hamiltonian can be simplified to

$$H = H_0 + V',$$

$$H_0 = \sum_{\alpha=0}^{n-1} \sum_k \omega_k |\alpha k\rangle\langle \alpha k| + \sum_{\alpha=0}^{n-1} \sum_{c=c_1,c_2} \omega_{\alpha c} |\alpha c\rangle\langle \alpha c|, \tag{3}$$

$$V' = \sum_\alpha \sum_{k,c} \left[V_{\alpha c,\alpha k} |\alpha c\rangle\langle \alpha k| + V_{\alpha k,\alpha c} |\alpha k\rangle\langle \alpha c| \right]$$

And $|\alpha c_1\rangle$ and $|\alpha c_2\rangle$ will be different from $|\alpha e\rangle$ and $|\alpha o\rangle$ because the mirror operations are not commutable with C_n. From this Hamiltonian, it is easy to calculate the forward and backward scattering amplitudes for $|\alpha k\rangle$. The backward scattering amplitude is proportional to the following expression and must vanish

$$A_{back} \sim G_{\alpha c_1,\alpha c_1} - G_{\alpha c_{c1},\alpha c_2} = 0. \tag{4}$$

Note $\bar{k} = -k$, and the Green's function is given by

$$G_{\alpha c_i,\alpha c_i} = \frac{1}{\omega - \tilde{\omega}_{\alpha c_i} + i\Gamma_{\alpha c}}, \quad i=1,2 \tag{5}$$

where $\tilde{\omega}_{\alpha c_i}$ is the modified cavity mode frequency incorporating a shift due to coupling to the waveguides, and $\Gamma_{\alpha c_i} = \sigma_{\alpha c_i} + \gamma_{\alpha c_i} \sigma_{\alpha c}$ represents loss intrinsic to the cavities, and $\gamma_{\alpha c}$ is attributed coupling to the waveguides. A general condition has been given under which the backscattering amplitude exactly vanishes.[11] Part of it still relies on the "accidental degeneracy", $\tilde{\omega}_{\alpha c_1} = \tilde{\omega}_{\alpha c_1}$, and $\Gamma_{\alpha c_1} = \Gamma_{\alpha c_2}$. However, usually it is difficult to satisfy these conditions *exactly* in simulation or design, even for an *n*=2 case. Nonetheless, simulations have shown that close to 100% forward transfer and almost zero backscattering is still achievable.[9] A special analysis is necessary in regard to how good the forward and backward transfer spectra are as a realistic system deviates from the ideal accidental degeneracy. Let

$$\Delta G(\omega_k) \equiv G_{\alpha c_1,\alpha c_1} - G_{\alpha c_{c1},\alpha c_2}. \tag{6}$$

It is straightforward to show that

$$|\Delta G(\omega)|^2 = \frac{\Delta\omega^2 + \Delta\Gamma^2}{[(\omega - \omega_1)^2 + \Gamma_1^2] \cdot [(\omega - \omega_2)^2 + \Gamma_2^2]}, \tag{7}$$

where for simplicity we let $\omega_i = \tilde{\omega}_{\alpha c_i}$, $\Gamma_i = \Gamma_{\alpha c_i}$, $\Delta\omega = \omega_2 - \omega_1$, and $\Delta\Gamma = \Gamma_2 - \Gamma_1$. The normalized backscattering intensity is proportional to

$$I_{back} \approx \gamma_1^2 |\Delta G(\omega)|^2.$$

Here we have neglected the difference between $\gamma_1 = \gamma_{\alpha c_1}$ and $\gamma_2 = \gamma_{\alpha c_2}$. In a passive system(*i.e.* no any electrical or optical power input other than the incoming wave in the input waveguide), the damping constants σ_i, γ_i, and Γ_i must be non-negative. Now it is straightforward to show that the maximum backscattering intensity, or strictly speaking an upper bound of the intensity, is given by

$$(I_{back})_{max} \approx \frac{\gamma_1^2 (\Delta\omega^2 + \Delta\Gamma^2)}{\Gamma_1^2 \Gamma_2^2} \leq \frac{\Delta\omega^2 + \Delta\Gamma^2}{\Gamma_2^2}. \tag{8}$$

With a bit more work, we shall be able to derive a more accurate bound, which will involve quite complicated terms like $max(\Gamma_1, \Gamma_2)$ or $min(\Gamma_1, \Gamma_2)$ and will also have more complicated dependence on $\Delta\omega$. However, it is usually sufficient to use Eq. (8) to estimate the backscattering intensity. Evidently, the upper bound given in Eq. (8) is relatively tolerant to the deviation from the accidental degeneracy. Even if both the frequency degeneracy and the linewidth degeneracy is violated by an amount as much as 10% of the value of the ideal linewidth, *i.e.* $\Delta\omega = \Delta\Gamma = 0.1\ \Gamma$, the normalized backscattering intensity cannot exceeding 1.7%. The actually number is usually even lower. Figure 2 illustrates such a case with 10% deviation in both center frequency and linewidth. The actual peak intensity of the backscattering spectrum is about 1.3%, lower than the predicted value. In calculating the intensity in Fig. 2(b), we have assume σ_i=0, otherwise, the peak of backscattering intensity will usually be even lower.
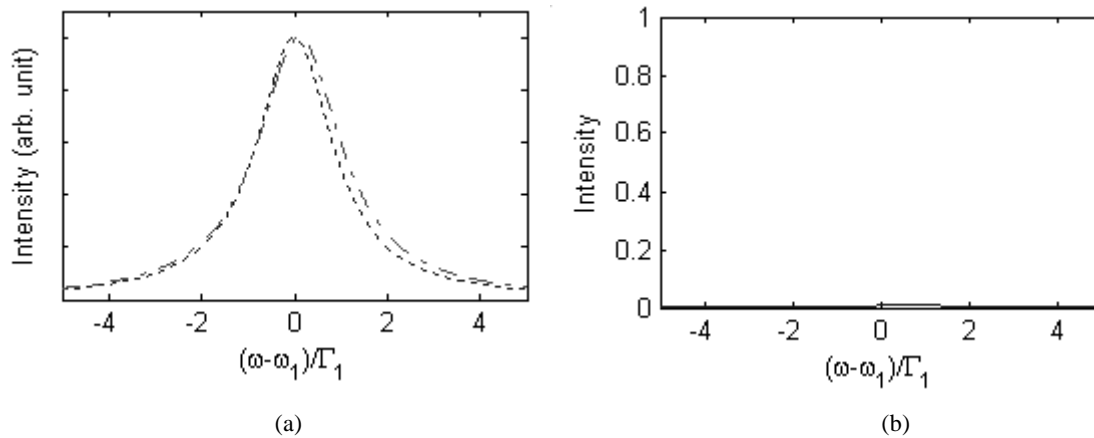
Fig. 2   Backscattering amplitude for imperfect accidental degeneracy: $\omega_2 - \omega_1 = \Gamma_2 - \Gamma_1 = 0.1\ \Gamma_1$. (a) Resonant spectra of the two cavity mode, (b) Normalized backscattering amplitude, the actual peak intensity of the backscattering spectrum is about 1.3%, lower than the predicted value 1.7%

In conclusion, we have shown that even the accidental degeneracy is not perfectly satisfied, a low backscattering intensity can still be maintained. This applies to a system with any n(including $n=2$). Apart from this, the full analysis of the channel drop processes in such a n-fold symmetric system can be found in Ref. [11].

3.   LIGHT REFRACTION AT A SURFACE OF A PHOTONIC CRYSTAL

3.1. Anomalous refraction: superprism effect

Light refraction at an interface between a photonic crystal and a homogeneous medium has been subject to extensive study recently.[15]   The refraction angle is found to depend on incident angle and wavelength sensitively("superprism" effect), which may be utilized for wavelength-division-multiplexing(WDM) applications. Furthermore, in some cases, the light beam refracts to the opposite side of the surface normal, which generally is expected only when the refractive index of one medium happens to be negative. This "negative refraction" phenomenon has been further studied in the context of building superlenses with photonic crystals.[16-17]

3.2. Difficulties of prior theories and simulation methods

The physics behind the abnormal refraction is related to the coupling of the incident light with the propagating modes of the photonic crystal. Although the light beam direction inside the PHOTONIC CRYSTAL can be fairly easily determined from the dispersion surface of the PHOTONIC CRYSTAL, the coupling amplitude of each excited mode has not been adequately studied. This is a critical issue that prevents any realistic design of a WDM demultiplexer from being accomplished. A variety of theoretical methods are available to calculate the light propagation in photonic crystals, including transfer matrices,[18] the scattering theory of dielectric sphere lattice,[19] and the internal field expansion method.[20] However, in these theories, the problem is formulated as calculating the transmission and reflection coefficients, R and T for a parallel surface slab, rather than for each surface. These calculations always include the effect of multiple reflections within the slab. The transmitted and reflected waves are a superposition of all internal reflection orders. Therefore, the coefficients R and T for the slab are an infinite sum of the products of single-interface transmission and reflection coefficients. This is adequate for the case of a wide beam and a thin slab, where the secondary beams generated by multiple reflections in the photonic crystal has a significant overlap in space, particularly on the exiting surface of the slab, as shown in Fig. 3(a). However, this is not adequate for the case that the beam width is relatively narrow, the refraction angle is large, and the slab is relatively thick. Even after a single round-trip reflection, the secondary beam may not overlap with the direct-through beam, as illustrated in Fig. 3(b). Therefore, one has to know the single interface transmission and reflection amplitudes. A more complicated case is illustrated in Fig. 3(c), where a number of single-interface refraction problems must be solved sequentially to obtain the final exiting beam. The

knowledge of *R*, *T* for single-interface refractions will be crucial to optimize device performance in many other cases. For instance, the solutions to the single interface refractions are needed to explore the proposed WDM demultiplexers with non-parallel front and back surfaces.[21] Note although the prior theoretical methods can calculate the effects due to internal reflections. They can only deal with the case of infinite times of reflections in a parallel surface slab, which is an automatic result of solving Maxwell's equation for the slab. Solving the single-interface refraction problem gives us more freedom to deal with non-parallel surface geometry, and any times of internal reflections.

Finite Difference Time Domain (FDTD) simulations are generally performed to study the non-parallel surface cases quantitatively. But such simulations are time consuming, and may become prohibitive for the cases of high wavelength and angular sensitivities. High wavelength sensitivity demands fine grids; high angular sensitivity requires a very wide incident beam so that the angular spread of the incident beam is small, and the wide beam leads to a large simulation region.

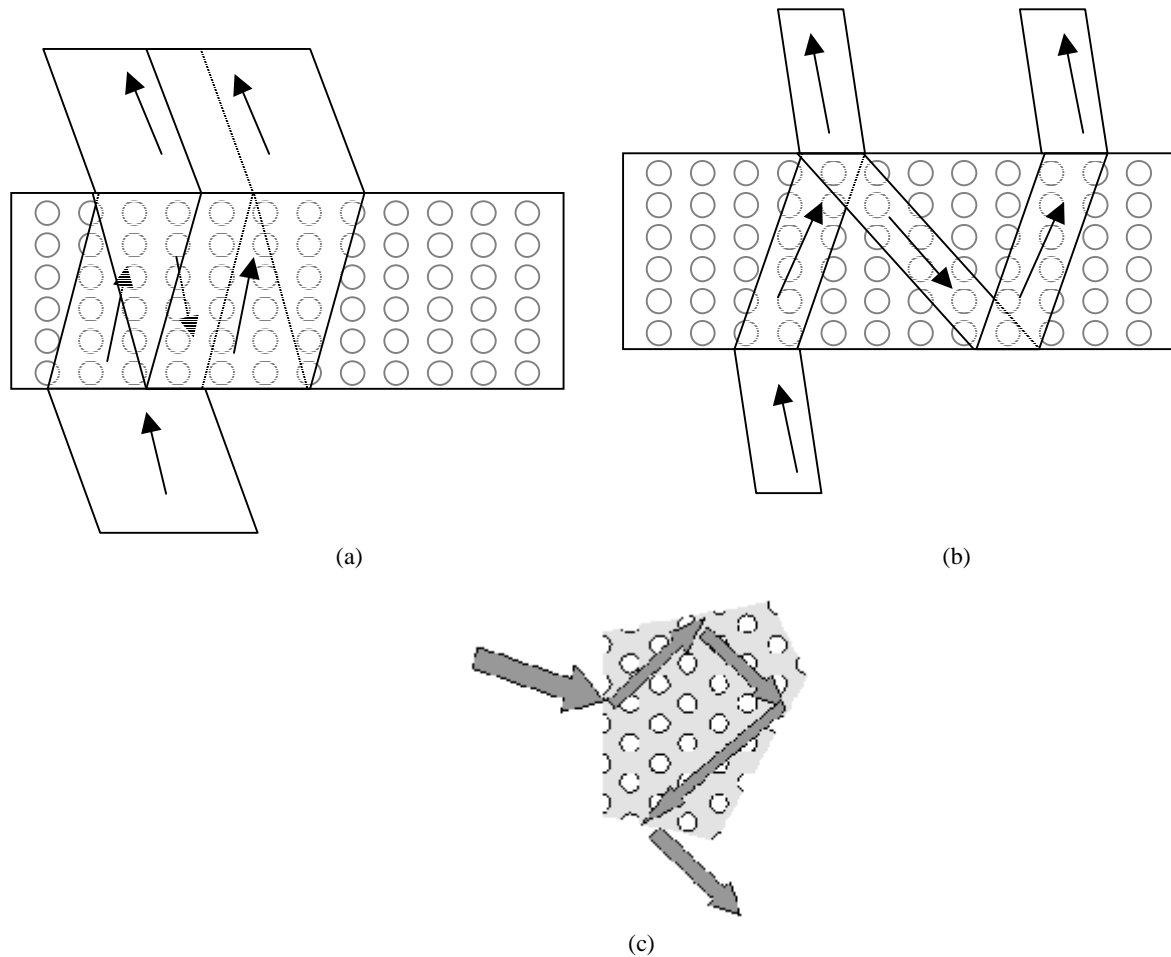(a)   (b)

(c)

Fig. 3 (a) Beams inside photonic crystal (and exiting beams) overlap significantly in space after a round-trip internal reflection inside a photonic crystal slab. A negative refraction case is presented, although the beam overlap/separation appears regardless of negative refraction. For simplicity, only one round-trip internal reflection is drawn. (b) Beams separate after one-round trip reflection. The single-interface refraction problem must be solved to obtain the intensity each of exiting beam. (c) Multiple internal reflections for non-parallel surfaces. Our theory can address all three cases. Conventional theory can only address case (a).

3.3. Theory for single-interface refraction problem
We have developed an analytic theory that not only solves the single-interface refraction problem, but also gives a physical picture of light refraction at the interfaces between photonic crystal and homogeneous

media. In addition, it provides an efficient way of calculating the relevant parameters of beam refraction, propagation in minimum time.

Our theory starts from the most widely used Bloch form of the photonic crystal modes and leads to a simple route of understanding the whole picture. It deals with a surface of photonic crystal with arbitrary orientation, which may be represented by an integer (or rational number) Miller index or by an irrational number Miller index. The latter actually implies that the surface is a quasi-periodic section of the 3D lattice.[22] Such a quasi-periodic surface structure usually demands more calculation resources. For the periodic surface structure, it will lead certain degeneracy of the photonic crystal modes when the reciprocal lattice is sectioned by the constant (k_x, k_y) line(k_x and k_y are wave vector components parallel to the surface). Rich intricacy has shown for this case, although we have found a way to sort out the degeneracy to identify the unique modes. The degeneracy is not solely due to the 3D periodicity in the Brillouin Zones replicated throughout the reciprocal space. In fact, 3D periodicity always exists, but the appearance of the degeneracy and the degree of the degeneracy depend on whether the Miller index of the surface are integers or irrational numbers, which will change for a same lattice as the surface orientation changes. Without understanding this degeneracy, the boundary condition can not be solved.

Another critical problem for the single interface problem is to separate the forward going refracted waves(i.e. the photonic crystal modes) and backward going refracted waves. Note the backward going refracted waves must be excluded in a single-interface problem when solving the boundary conditions. It is rather difficult to identify these two types of modes from the original set of linear equations for the Fourier coefficients of electric and magnetic fields. Nonetheless, by considering the topology[23] of the dispersion surface, a simple partition scheme is available. We proved the relation between the numbers of forward and backward refracted waves. Furthermore, we can address the beam width transformation and insertion loss for a Gaussian beam with sufficient accuracy. And we have applied this to design a polygon-shaped low-loss demultiplexer with many dense WDM channels.

4. NANO-FABRICATION OF PHOTONIC CRYSTALS

4.1. Electron beam lithography for nano-fabrication of photonic crystals

Photonic crystals are periodic structures with feature sizes comparable to the wavelength of light. For communication wavelengths around 1.55 μm, the feature sizes lie in the submicron range, which presents a challenge to the conventional photolithography techniques. Electron beam lithography is usually employed to pattern photonic crystals for visible and infrared wavelengths. We have used electron beam lithography to pattern structures on polymer films to fabricate two-dimensional(2D) photonic crystals. Several suits of electron beam lithography tools are available at the University of Texas at Austin. Some nano-lithography facilities at the University of Texas at Austin are shown in Fig. 4.

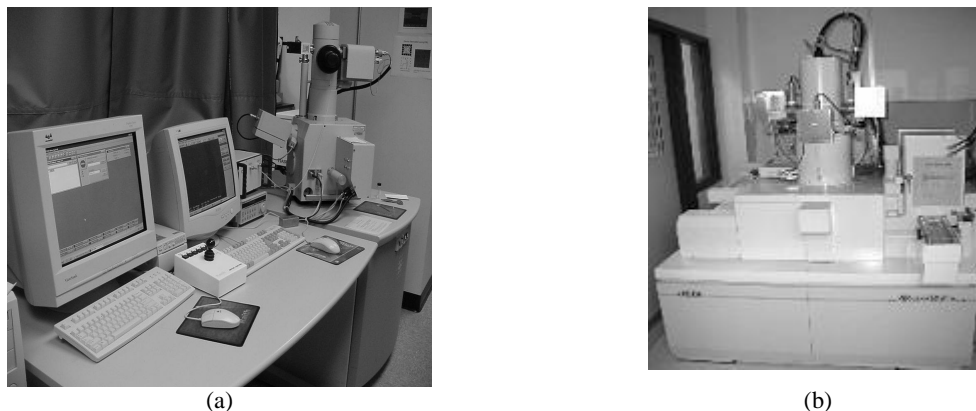(a)   (b)

Fig. 4 (a) Electron beam nanolithography facility at (a) Center for Nano- and Molecular Science Technology, (b) Microelectronics Research Center, both part of the University of Texas at Austin.

We have integrated photonic crystals and conventional channel waveguides on a multi-layer polymer film. First, the bottom cladding layer and core layer of the waveguides are spin-coated on a silicon wafer. Conventional photolithography is employed to pattern the waveguide core layer, followed by reactive ion etching(RIE). Subsequently, the top cladding layer is applied. By careful design and fabrication, the top surface of the polymer film stack can usually be planarized easily despite the undulating core layer underneath. The planarization of the top surface is important for the successful patterning by electron beam lithography that follows because the depth of focus of the electron beam is usually fairly small. A segment of photonic crystal fabricated on a polymer multi-layer film is shown in Fig. 5. We are able to achieve holes of very high aspect ratios around 7:1 with hole radii in the submicron range. Optical tests show that the out-of-plane radiation loss[24-25] for the short segment of holes shown in Fig. 5 is low. We compare a straight waveguide and a waveguide with this short segment of photonic crystal inserted in the middle of its length, the difference in insertion loss is on average below 1dB, with a variation from 0 to 3 dB. The loss and loss variation are attributed to a number of factors, including the roughness of holes' walls, hole size uniformity, out-of-plane loss, and polymer curing conditions. Further improvement is underway. Detailed analysis of the origin of the loss will be presented elsewhere.
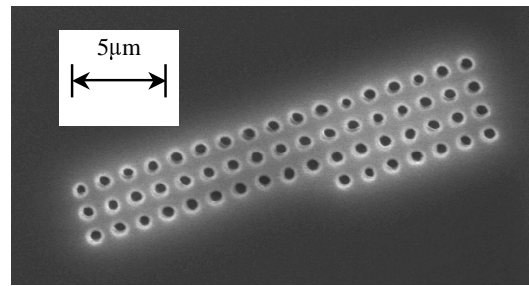

Fig. 5 A segment of photonic crystal fabricated on a multi-layer polymer film.

5. ACKNOWLEDGEMENT

REFERENCES

1. E. Yablonovitch, *Phys. Rev. Lett.*, **58**,1059,(1987).
2. S. John, *Phys. Rev. Lett.*, **58**,12486,(1987).
3. O. Painter, R. K. Lee, A. Scherer, A. Yariv, J. D. O'Brien, D. P. Dapkus, I. Kim, "Two-dimensional photonic band-gap defect lasers," Science, vol. 284, pp. 1819 (1999).
4. T. Yoshie, O. B. Shchekin, H. Chen, D. G. Deppe, and A. Scherer, "Quantum dot photonic crystal lasers," Electronics Letters, vol. 38, pp. 967 (2002).
5. A. Mekis, J. C. Chen, I. Kurland, S. Fan, P. R. Villeneuve, J. D. Joannopoulos, "High transmission through sharp bends in photonic crystal waveguides," Phys. Rev. Lett., vol.77, 3787, 1996.
6. S.-Y. Lin, E. Chow, V. Hietala, P. R. Villeneuve, and J. D. Joannopoulos, "Experimental demonstration of guiding and bending of electromagnetic waves in a photonic crystal," Science, vol. 282, 274 (1998).
7. M. Notomi, K. Yamada, A. Shinya, J. Takahashi, C. Takahashi, and I. Yokohama, "Extremely Large Group-Velocity Dispersion of Line-defect Waveguides in Photonic Crystal Slabs," Physical Review Letters, vol. 87, 253902 (2001).
8. K. Hosomi and T. Katsuyama, "A dispersion compensator using coupled defects in photonic crystals," IEEE J. Quantum Electronics, vol. 38, 825 (2002).
9. S. Fan, P. R. Villeneuve, J. D. Joannopoulos, and H. A. Haus, Phys. Rev. Lett., vol. 80, 960 (1998).

10. S. Fan *et. al.*, Phys. Rev. B vol. 59, 15882 (1999).
11. W. Jiang and R. T. Chen, "Multichannel optical add-drop process in symmetrical waveguide-resonator systems," *Phys. Rev. Lett.*, vol. 91, pp. 213901 (2003).
12. M. Hamermesh, *Group Theory and Its Application to Physical Problems* (Addison-Wesley, Reading, 1962).
13. J. Q. Chen, Group representation theory for physicists, World Scientific, Singapore, 1989.
14. Y. Xu, Y. Li, R. K. Lee, and A. Yariv, Phys. Rev. E vol. 62, 7389 (2000).
15. H. Kosaka, et. al., Phys. Rev. B, vol. 58, 10096 (1998).
16. M. Notomi, Phys. Rev. B, vol. 62, 10696, (2000).
17. C. Luo, S. G. Johnson, J. D. Joannopoulos, Phys. Rev. B, vol. 65, 201104 (2002).
18. J. B. Pendry and A. MacKinnon, Phys. Rev. Lett. vol. 69, 2772 (1992).
19. N. Stefanou, V. Yannopapas, and A. Modinos,Comput. Phys. Commun., vol, 132, 189 (2000).
20. K. Sakoda, Phys. Rev. B, vol. 52, 8992 (1995).
21. T. Baba and M. Nakamura, J. Quantum Electron., vol. 38, 909 (2002).
22. A. L. Mackay, Physica A, vol. 114, 609 (1982).
23. L. C. Kinsey, Topology of surfaces, (Springer-Verlag, New York, 1993).
24. H. Benisty, P. Lalanne, S. Olivier, M. Rattier, C. Weisbuch, C. J. M. Smith, T. F. Krauss, C. Jouanin, and D. Cassagne, Opt. Quantum Electron. 34, 205 (2002).
25. R. Ferrini, B. Lombardet, B. Wild, R. Houdre, and G.-H. Duan, Appl. Phys. Lett. Vol. 82, 1009, (2003).